Electronic Supplementary Material (ESI) for Soft Matter.

Self-assembly of Donor-acceptor Conjugated Polymers Induced by Miscible ‘Poor’ Solvents

Yuyin Xi, Caitlyn M. Wolf and Lilo D. Pozzo*

Department of Chemical Engineering, University of Washington, Seattle, WA 98195

Email: dpozzo@uw.edu

Supporting Information

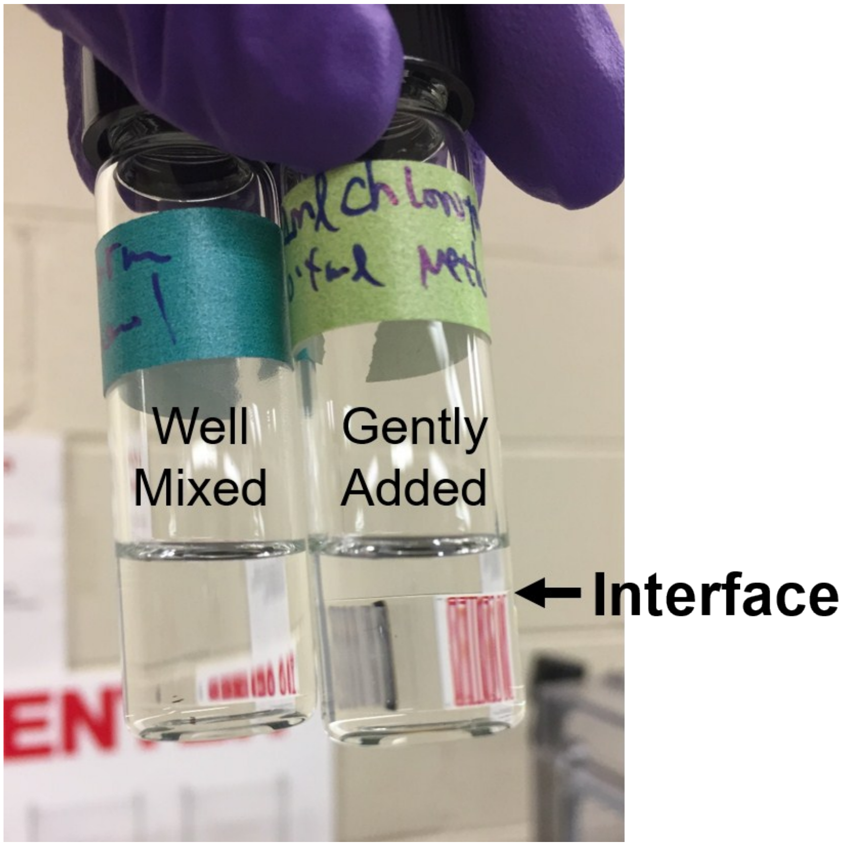

Figure S1. 16.7 v% methanol added into chloroform. After methanol is gently added, a clear sign of mixing is first observed of variation of density across the whole bulk solution. After a few seconds, an interface is formed. By simply shaking the solution with hand, the two layers of solution can be well mixed, which is shown in the left vial.

Table S1. Summary of lot number, molecular weight and dispersities of polymers.

Polymers	Lot #	M_w	$Đ$
DPPDTT	M315	279 k	3.65
PCDTPT	YY9100 & YY11066	76 k	2.5
PFT-100	YY8224P1	50 k	3
PCDTBT	MKBJ8073V	52 k	5.38

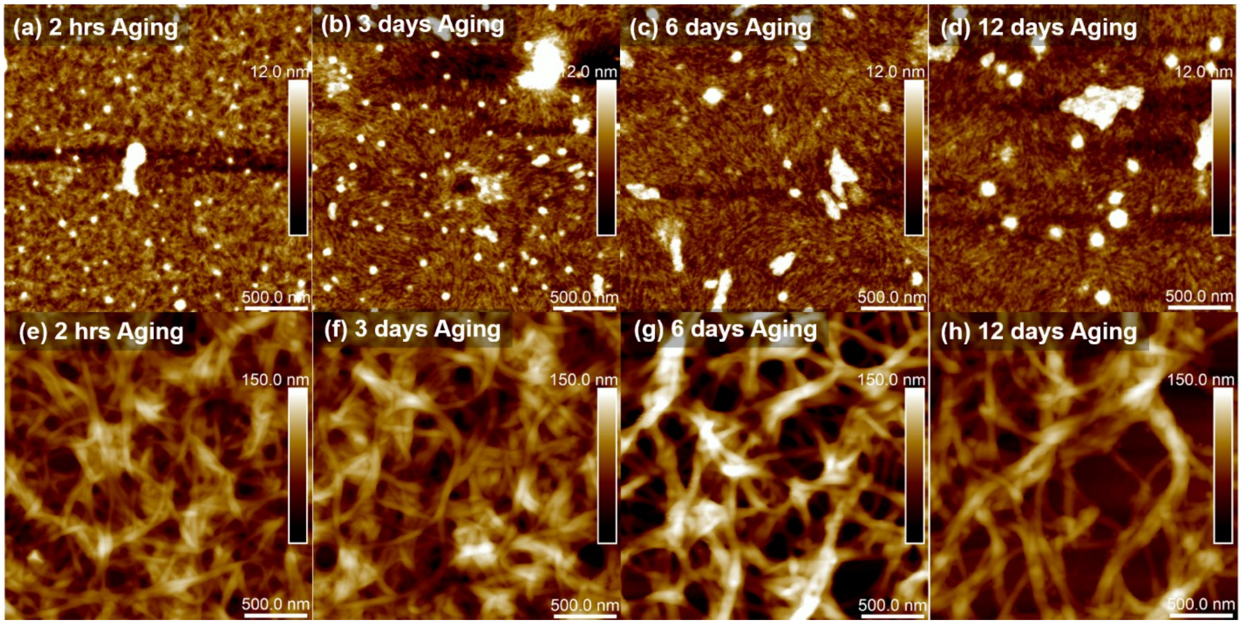

Figure S2. AFM images of 1.6 mg/ml DPPDTT in chloroform mixed with (a) (b) (c) (d) 10 v% methanol and (e) (f) (g) (h) 20 v% methanol after aging for (a) (e) 2 hrs, (b) (f) 3 days, (c) (g) 6 days, (d) (h) 12 days.

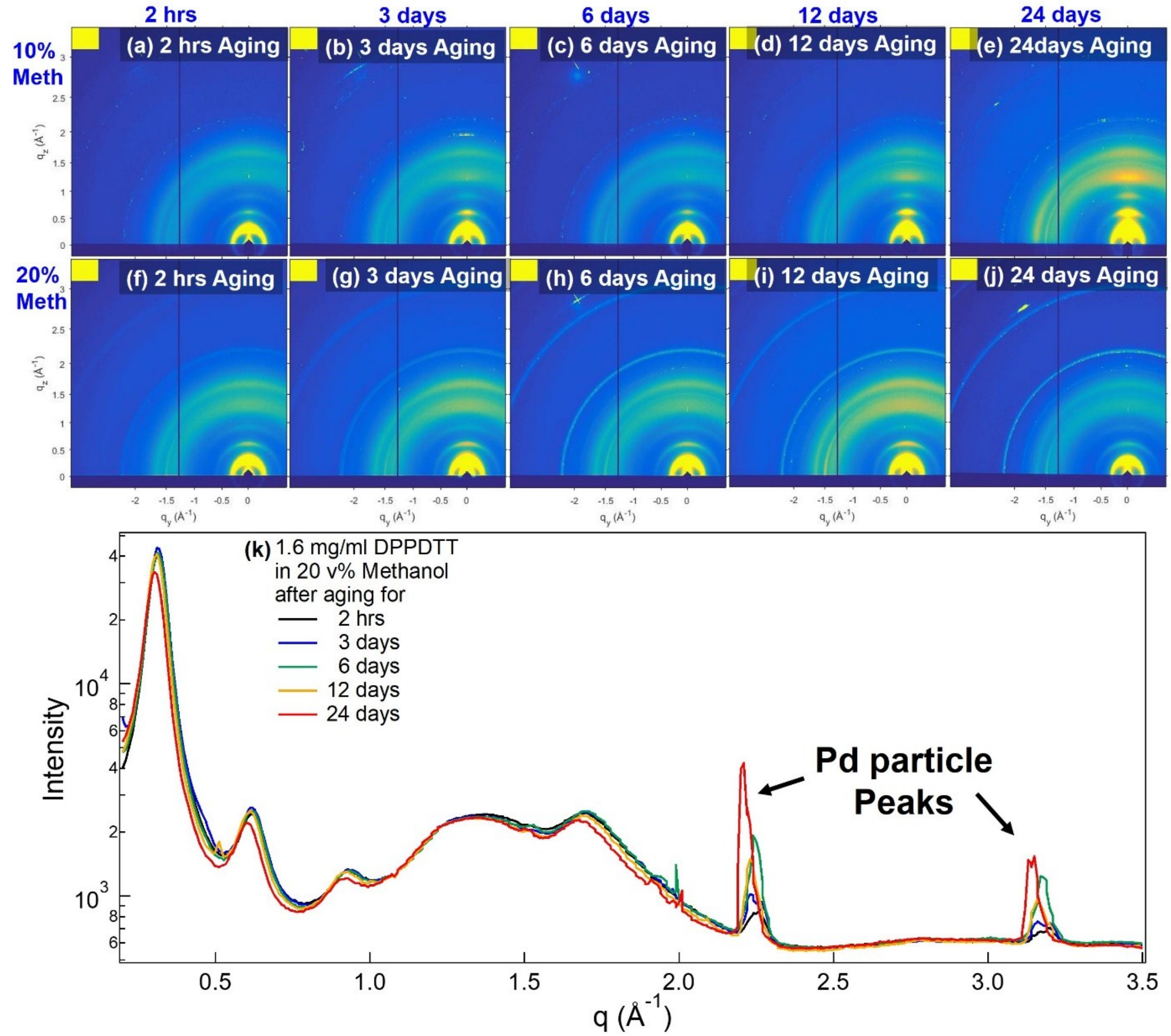

Figure S3. The corresponding 2-D GIWAXS pattern of the samples in Figure S1 of 1.6 mg/ml DPPDTT in chloroform mixed with (a) (b) (c) (d) (e) 10 v% methanol and (f) (g) (h) (i) (j) 20 v% methanol after aging for (a) (f) 2 hrs, (b) (g) 3 days, (c) (h) 6 days, (d) (i) 12 days, (e) (j) 24 days. (k) Reduced 1-D profiles in the out-of-plane direction (φ=105˚ with 5˚ integration angle).

Figure S4 shows sTEM image and electron diffraction pattern on the nanoparticles and nanoribbons. The formation of the nanoparticles is attributed to the Pd catalyst contaminates from the polymer samples. The generation of Pd nanoparticles are visible under sTEM for some of our samples. Electron diffraction on the nanoparticles spot show that the nanoparticles are very crystalline in comparison to the nanoribbons. It is possible that the addition of methanol caused the reduction of residual catalyst leading to the formation of Pd nanoparticles. The (110) face of Pd crystal matches with the peak at q=2.2 Å^{-1} and (200) face corresponds to the peak at q=3.2 Å^{-1}.

Although Pd nanoparticles exhibit well-defined peaks at high q-range, no evidence that palladium particles affect or interference with the low-q scattering data (SANS and low-q GIWAXS) from polymers was noticed. In GIWAXS data, only the high-q peaks at q=2.2 Å^{-1} and 3.2 Å^{-1} grow with aging when methanol is added (Figure S3) and nanoparticles are formed. All the other polymer peaks and features stay the same as a function of aging. This indicates that the generation of Pd particles does not alter the polymer peaks. With respect to SANS experiments, the neutron scattering contrast between the hydrogenated polymer molecules and the deuterated chloroform is about one order of magnitude larger than that between palladium particles and the solvent. Moreover, the much larger size of the polymer structures that are formed (i.e. micrometers long), as compared to the Pd nanoparticles (~10 nm), leads to total dominance of the scattering at very low angles (SANS region) by the conjugated polymer.

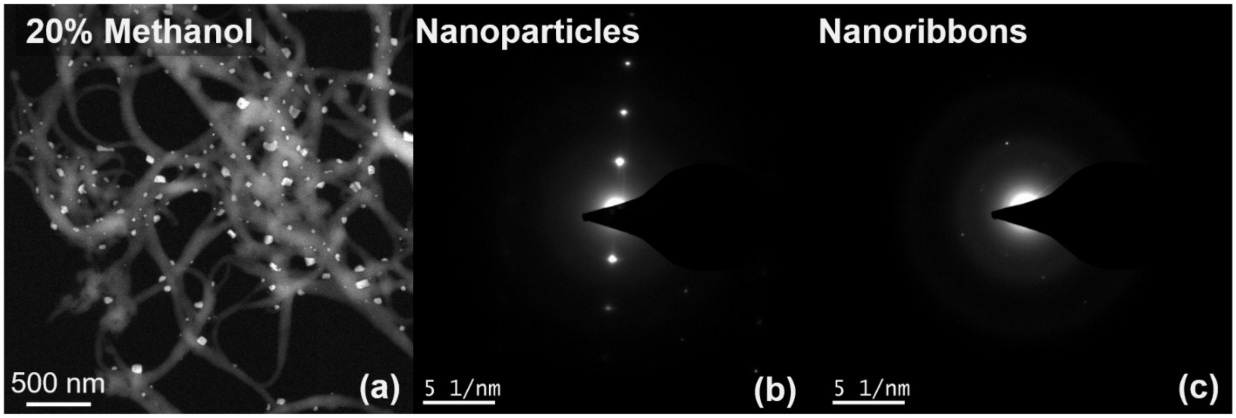

Figure S4 (a) sTEM image of 1.6 mg/ml DPPDTT with 20 vol% methanol. Electron diffraction patterns on (a) nanoparticles and (b) nanoribbons.

The dielectric constant measurement was achieved by using an Anton Paar MCR 301 stress controlled rheometer. The detailed experimental set up is described in our previous publication. [1]

Basically, a 25 mm parallel plate geometry was used to define a gap of 250 μm. A solvent trap was used to prevent the solvent from evaporating. A gold wire was used to connect the upper plate shaft and the bottom plate to a Agilent e4980 LCR meter. A frequency sweep between 20 Hz and 1 MHz with a 20 mV perturbation voltage was used to obtain the dielectric constant of different mixtures.

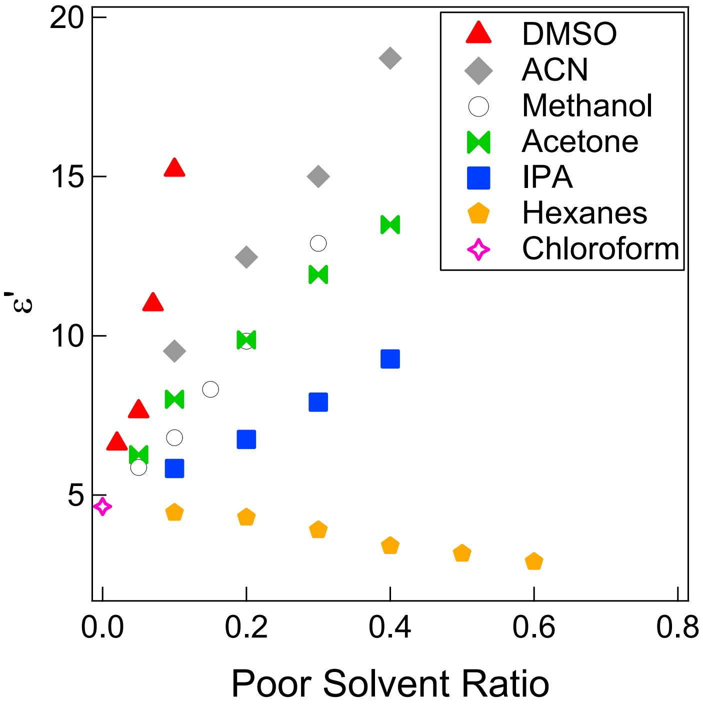

Figure S5. Measured dielectric constant of chloroform mixture with various poor solvents of different ratios.

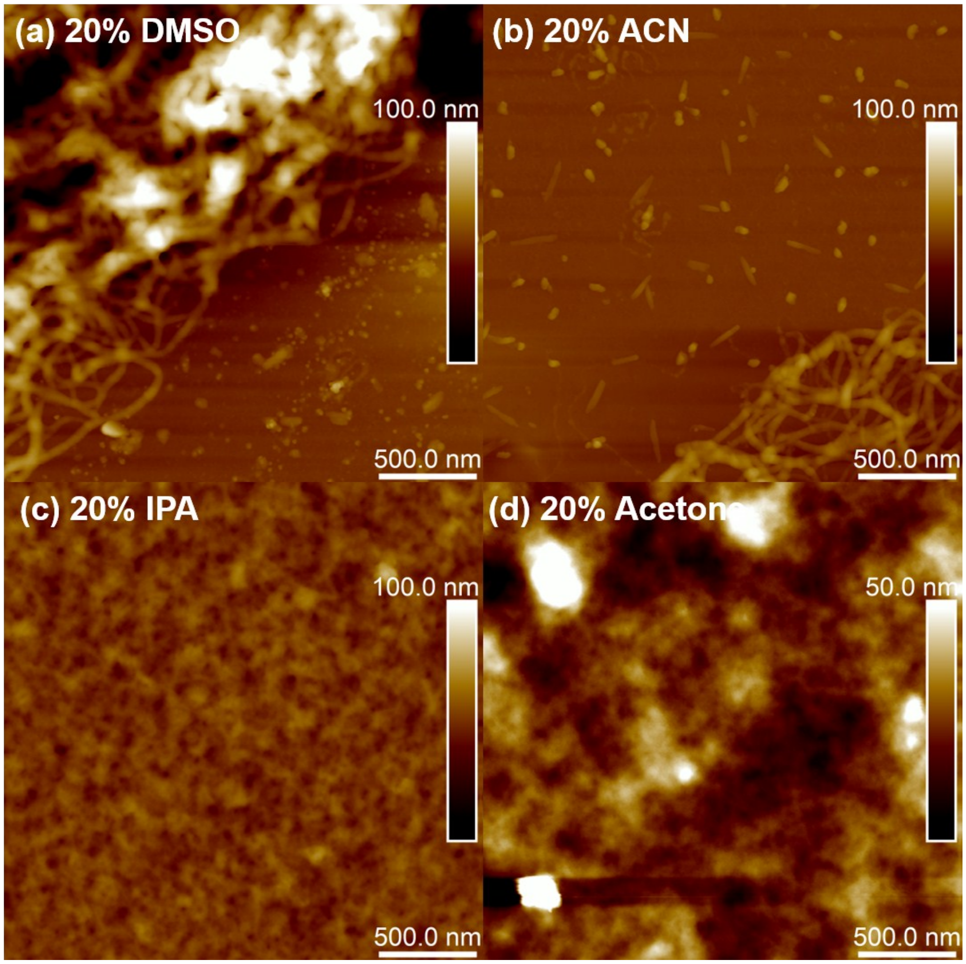

Figure S6. AFM images of 1.6 mg/ml DPPDTT in chloroform mixed with 20 v% (a) DMSO (b) Acetonitrile (ACN) (c) IPA (d) Acetone. The samples were cast after preparation without aging.

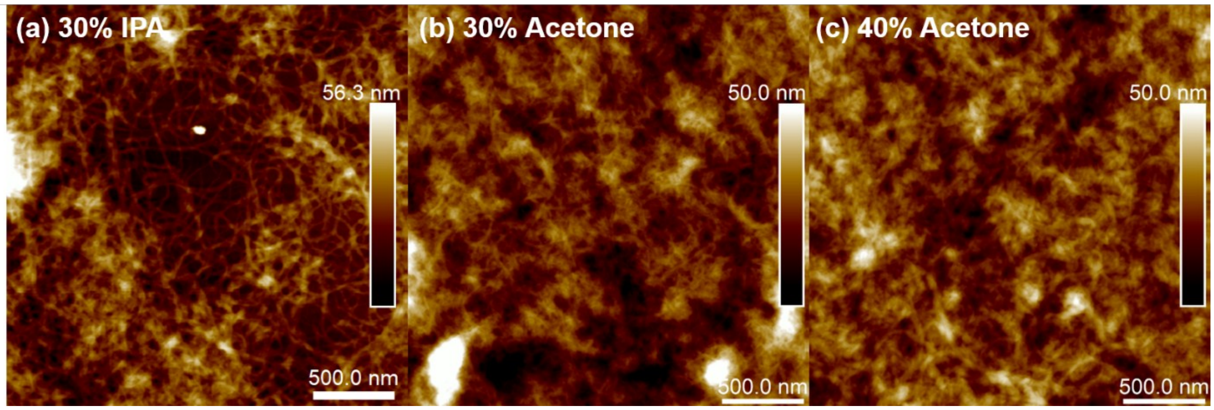

Figure S7. AFM images of films spin coated from1.6 mg/ml DPPDTT mixed with (a) 30 v% IPA, (b) 30 v% acetone and (c) 40 v% acetone. The samples are cast within a day after preparation.

In this manuscript, two models were used to quantify polymer nano-structures and conformations. The semi-flexible cylinder model is used to model all polymers in dissolved states. The combined model of parallelepiped and dissolved polymers is used for systems that have also clearly started to self-assemble into nanoribbons but still contain ‘free’ dissolved polymer in equilibrium. At low methanol concentrations (below 15 v%), no clear sign of self-assembly into nanoribbons is observed, so these samples are modeled with a flexible cylinder model to probe the polymer conformation. For high methanol concentration (20 vol%) and those with DMSO and acetonitrile that clearly form nanoribbons, a combined model (i.e. ribbons plus dissolved polymer) is used to quantify the cross-sectional size of the ribbons and the relative amount of polymer that is found in nanoribbons. More detailed description of each model is presented below.

Description of combined model of parallelepiped and dissolved polymers with excluded volume effect.

Polymer nanoribbons were modeled with parallelepiped model [2,3] combined with dissolved polymer model considering excluded volume effect [4,5]. The fraction of parallelepiped model (φ_f) indicates the amount of polymers that form nanoribbons. The form factor of the combined model is depicted in Eq-S1.

$$I\,(q) = \phi_v \varphi_f (\Delta\rho)^2 P_{PP}(q) + \phi_v (1 - \varphi_f)(\Delta\rho)^2 P_{PExV}(q) \qquad \text{Eq-S1}$$

Where the total volume fraction of conjugated polymers in solution is denoted by ϕ_v, $\Delta\rho$ is the scattering length density (SLD) difference between solvent and polymer chains. $P_{PP}(q)$ represents the form factor of the parallelepiped model and $P_{PExV}(q)$ is that of dissolved polymers with excluded volume effect. Both of the form factors are defined in Eq-S2~ S5.

$$P_{PP}(q) = \frac{2}{\pi}\int_{0}^{2\pi}\int_{0}^{2\pi}\left[\left(\frac{\sin(qA\sin\alpha\cos\beta)}{qA\sin\alpha\cos\beta}\right)\left(\frac{\sin(qB\sin\alpha\cos\beta)}{qB\sin\alpha\cos\beta}\right)\left(\frac{\sin(qC\cos\alpha)}{qC\cos\alpha}\right)\right]^{2}\sin\alpha d\alpha d\beta \qquad \text{Eq-S2}$$

$$P_{PExV}(q) = \frac{1}{\nu U^{\frac{1}{2\nu}}}\gamma\left(\frac{1}{2\nu},U\right) - \frac{1}{\nu U^{\frac{1}{\nu}}}\gamma\left(\frac{1}{\nu},U\right) \qquad \text{Eq-S3}$$

$$\gamma(x,U) = \int_{0}^{U} dt\, exp(-t)t^{x-1} \qquad \text{Eq-S4}$$

$$U = \frac{q^{2}R_{g}^{2}(2\nu+1)(2\nu+2)}{6} \qquad \text{Eq-S5}$$

Where a and b are the width and height of the parallelepiped, and c denotes the length of the nanoribbons. As the length of the nanoribbon is over one micrometer, which is outside of the windown that SANS is probing. The length C of the model is fixed at 1 μm for all the samples. R_g is the radius of gyration of fully dissolved polymers and ν represents excluded volume paramter, which is the inverse of Porod exponent.

Description of flexible cylinder model with excluded volume effect

For flexible cylinder, each polymer chain is modeled with a contour length of L and a radius of b. Each polymer chain can be viewed as several rigid rods that are combined. The length of each rigid rod is called persistent length (l_p). Kuhn length (b) is defined as two times of persistent length, which reflects the rigidity of a polymer chain. The scattering intensity using flexible cylinder form factor can be modeled with concentration (c), SLD difference ($\Delta\rho$), and molecular weight (M) as shown in equation S6. [6,7] The scattering functions of single semiflexible chain ($S(q,L,b)$) considering polydispersity of contour length and cross section of a rigid rod ($P(q,r)$) are defined from equation S7 to equation S18.

$$I(q, L, b, r) = c\Delta\rho^2 M < S(q,L,b) >_{SZ} P(q,r) + bkg$$ Eq-S6

$$P(q,r) = [\frac{2J_1(qr)}{qr}]^2$$ Eq-S7

$$< S(q,L,b) >_{SZ} = \frac{\int N_{SZ}(L) L^2 S(q,L,b) dL}{\int N_{SZ}(L) L^2 dL}$$ Eq-S8

$$N_{SZ}(L) = \frac{L^z}{z!}(\frac{z+1}{< L >})^{z+1} exp[\frac{-L(z+1)}{< L >}]$$ Eq-S9

$$S(q,L,b)$$
$$= [1 - w(qR_G) S_{Debye}(q,L,b) + w(qR_G)\left[1.22(qR_G)^{-\frac{1}{0.585}} + 0.4288(qR_G)^{-\frac{2}{0.585}} + 1.651(qR_G)^{-\frac{3}{0.585}}\right]$$
$$\{\frac{4}{15} + \frac{7}{15u} - (\frac{11}{15} + \frac{7}{15u}) \times exp[-u(q,L,b)]]\}$$ Eq-S10

$$S_{Debye}(q,L,b) = \frac{2}{u(q,L,b)}\{\exp[-u(q,L,b)] + u(q,L,b) - 1\}$$ Eq-S11

$$u(q,L,b) = \frac{Lb}{6}\{1 - \frac{3}{2n_b} + \frac{3}{2n_b^2} - \frac{3}{4n_b^3}[1 - exp(-2n_b)]\}q^2$$ Eq-S12

$$n_b = \frac{L}{b}$$ Eq-S13

$$w(x) = \frac{\{1 + tanh[(x - 1.523)/0.1477]\}}{2}$$ Eq-S14

$$< R_G^2 >= \alpha(n_b)^2 \frac{bL}{6}$$ Eq-S15

$$u(q,L,b) = \alpha(n_b)^2 q^2 \frac{bL}{6}$$ Eq-S16

$$\alpha(x) = \sqrt{[1 + \left(\frac{x}{3.12}\right)^2 + (\frac{x}{8.67})^3]^{0.176/3}}$$ Eq-S17

$$C(n_b) = \begin{matrix} 3.06 n_b^{-0.44} & for\ L > 10b \\ 1 & for\ L \le 10b \end{matrix}$$ Eq-S18

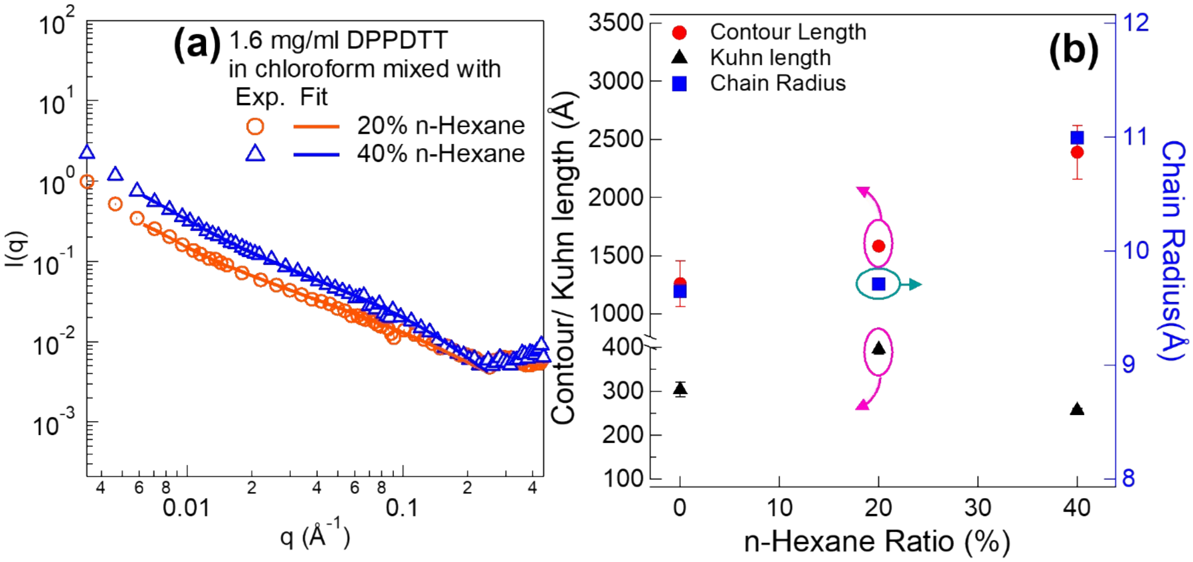

Figure S8. (a) SANS profiles of DPPDTT with 20 v% and 40 v% n-Hexane. The profiles are fit with flexible cylinder model. (b) The extrapolated contour length, Kuhn Length, and radius from the model.

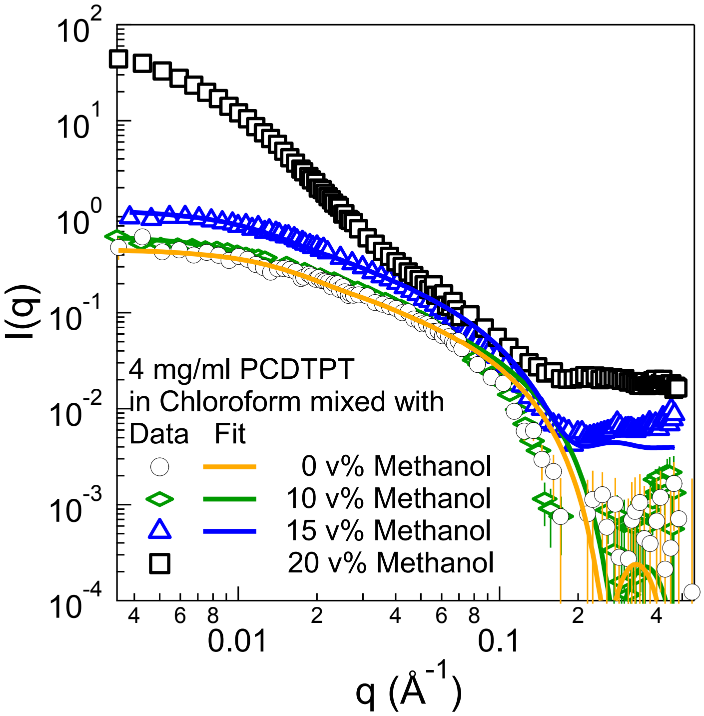

Figure S9. 1D SANS scattering profile of 4 mg/ml PCDTPT in chloroform mixed with varied methanol concentrations. A cylinder model was used to fit the SANS profiles at low methanol concentrations.

Table S2. Extrapolated fitting parameters for PCDTPT samples from a cylinder model.

Methanol Ratio	**Radius (nm)**	**Length (nm)**
0v%	1.5	30.0
10v%	1.4	39.6
15v%	1.8	38.4

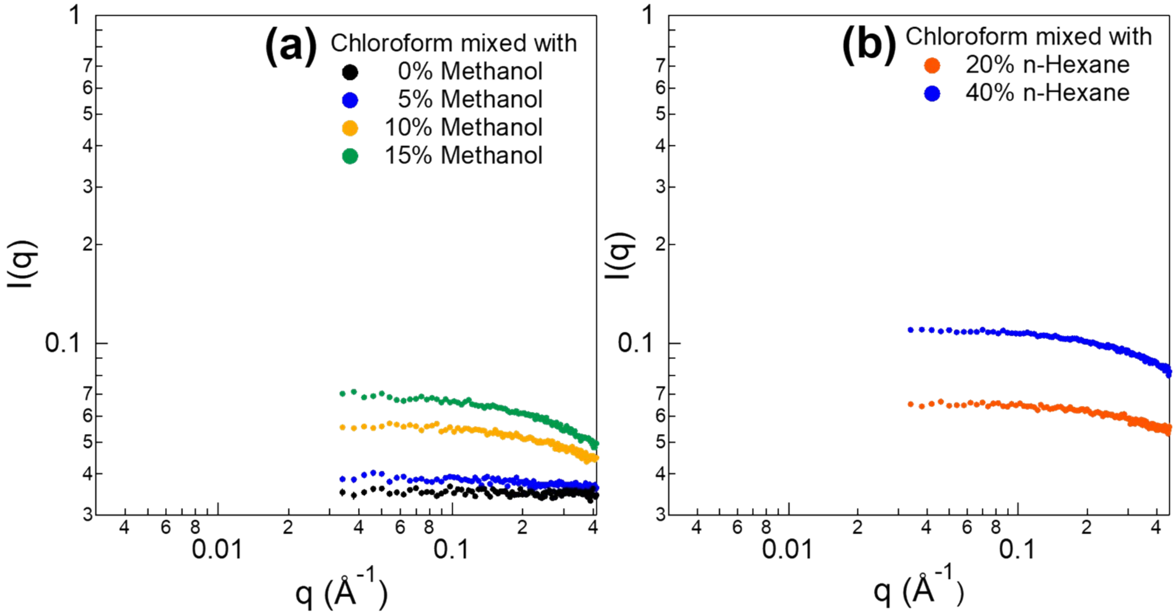

Figure S10. 1-D SANS scattering profiles of d-chloroform mixed with (a) d4-methanol and (b) d14-n-hexane with different ratios.

(1) Xi, Y.; Pozzo, L. D. Electric Field Directed Formation of Aligned Conjugated Polymer Fibers. *Soft Matter* **2017**, *13*, 3894–3908 DOI: 10.1039/C7SM00485K.

(2) Roman Nayuk, K. H. Formfactors of Hollow and Massive Rectangular Parallelepipeds at Variable Degree of Anisometry. *Zeitschrift für Phys. Chemie* **2012**, *226*, 837–854.

(3) P. Mittelbach, G. P. X-Ray Low-Angle Scattering by Dilute Scattering Colloidal Systems. The Calculation of Scattering Curves of Parallelepipeds. *Acta Phys. Austriaca* **1961**, *14*, 185–211.

(4) H. Benoit. La Diffusion de La Lumiere Par Des Macromolecules En Chaines En Solution Dans Un Bon Solvant. *Comptes Rendus* **1957**, *245*, 2244–2247.

(5) Hammouda, B. SANS from Homogeneous Polymer Mixtures - A Unified Overview. *Adv. Polym. Sci.* **1993**, *106*, 87–133.

(6) Pedersen, J. S.; Schurtenberger, P. Scattering Functions of Semiflexible Polymers with and without Excluded Volume Effects. *Macromolecules* **1996**, *29* (23), 7602–7612 DOI:

10.1021/ma9607630.

(7) Chen, W.-R.; Butler, P. D.; Magid, L. J. Incorporating Intermicellar Interactions in the Fitting of SANS Data from Cationic Wormlike Micelles. *Langmuir* **2006**, *22* (15), 6539–6548 DOI: 10.1021/la0530440.